Science, Engineering & Education, 9, (1), 2024, 115-122

Laboratory Determination of Absorption Refrigeration Cycles

Yordan Stoyanov, Nina Penkova*, Kalin Krumov

University of Chemical Technology and Metallurgy, 8 Kliment Ohridski Blvd., Sofia 1797, Bulgaria

Received 24 June 2024, Accepted 30 July 2024
DOI: 10.59957/see.v9.i1.2024.16

ABSTRACT

A methodology for experimentally particularizations and analyses of thermodynamically cycles of the binary mixture at laboratory diffusion absorption refrigerators is developed. It allows estimation of the performances of the unit at cooling and heat pump mode for scientifically and education purposes. The developed approach will be used to educate students in the courses of thermodynamics and renewable energy systems about the applications of the absorption cycles for utilisation of solar or waste energy for cold and heat production.

Keywords: diffusion absorption refrigerator, thermodynamically cycle, heat pump, performance, experimental study.

INTRODUCTION

The diffusion absorption refrigerators (DAR) have been developed in 1928 by Von Platen and Munters [1]. These systems can be thermally driven by solar or waste thermal energy at negligible electricity consumption and can generate cold or heat for domestic and industrial purposes [2 - 6]. Their operations are quiet and associated with low operating costs. Due to these advantages, the absorption refrigeration technologies are continuously evolving for a variety of applications [7 - 10]. At the same time, the thermodynamically and transport phenomena in the binary solutions in DAR are complex and actual to study.

An absorption refrigeration laboratory system was funded by project КП-06 Н57/16/2021 "Parametric analysis of multiphysical processes in absorption refrigeration systems for efficient utilization of thermal energy" and supplied in University of Chemical Technology and Metallurgy (UCTM). Absorption cycles at variable power inputs were investigated to obtain detail information about the different thermodynamically states of the binary mixture and to estimate the efficiencies and the operation range of DAR [11]. In addition to scientific activities, the laboratory installation can be used for the engineering education in UCTM. A methodology for determining the thermodynamically states and cycles of the binary solution and the efficiency of the DAR at refrigeration and heat pump modes for educational purposes is developed and demonstrated in this study.

Correspondence to: Nina Penkova, University of Chemical Technology and Metallurgy, 8 Kliment Ohridski Blvd., Sofia 1797, Bulgaria, E-mail: nina@uctm.edu

EXPERIMENTAL

Laboratory absorption refrigeration system

The laboratory DAR, shown of Fig. 1 and Fig. 2, is made by Edibon [12]. It is thermally driven by an electrical heater with a rated power of 120 W. There are capabilities for variation of the input electrical power. A gas burner is an additional option for energy supply in the generator.

The binary mixture is consisted of ammonia (refrigerant) and water (absorbent). Its states between the elements of the system are numbered and pointed on Fig. 1 and Fig. 3, accepting a signing as follows: prime symbol for saturated liquid, double prime symbol for saturated steam and "o" for wet vapour. The non-boiling liquid states are pointed as numbers without additional elements.

The rich of ammonia solution inflows in the generator (state 1o), absorbs thermal energy, released by the electrical heater and boils to state 2o of wet vapour. This vapour is consisted of saturated steam (state 2") and liquid (state 2') on the generator outlet. The steam bubbles, formed during the boiling rise up, entraining the liquid. This creates a thermosiphon or bubble pump effect, which moves the solution through the elements of the refrigerator.

The steam (state 2") enters the condenser, where the ammonia condenses at pressure p_c, releasing a heat flow to the room environment. The liquid in state 2' flows down to the "pipe in pipe" heat exchanger, where it exchanges heat with the ammonia-rich solution, flowing from the absorber to the generator in state 4. The poor of ammonia liquid, cooled to state 3, enters the absorber, where it absorbs the ammonia vapour.

The liquid and subcooled ammonia after the condenser is throttled from state 5o to state of wet vapour 6o. The throttling reduces its pressure to p_e. After the expansion pipe, the wet vapour enters the evaporator, where it evaporates to the state 7o at nearly constant pressure and temperature, absorbing a heat flow from the freezing chamber. That vapour is then heated in the cooling chamber to state 8o, mixed with the non-condensed vapour (5") and enters the absorber, where it is absorbed by the ammonia-poor liquid solution. The rich of ammonia solution is heated in the heat exchanger from state 4 to state 9 and partially boils to state 1o, as it is established during the experiments. A heat flow is released to the environment during the absorption.

Ten sensors (ST1-ST10) measure important temperatures of the binary solution, the cooled and the heated environments. That allow fixing the states of the solution, determining the processes in thermodynamically charts and computing of energy parameters of DAR.

A steady state has to be obtained at a fixed power input P before the measuring process. It is achieved at continuous operation of the unit about one hour. The measuring steps, assumptions and computations to determine the states and the processes of the binary mixture are demonstrated in Table 1.

The estimations of the thermodynamic parameters of the binary solution are implemented at the following assumptions [11]:

- the refrigerator operates continuously;
- the heating and boiling in the generator and the condensation in the condenser are isobaric processes and proceed at pressure p_c;
- the water does not condense in the condenser;
- the evaporation in the evaporator proceeds at constant pressure p_e;
- the thermal losses to the environment at the generator and the heat exchanger are negligible.

Energy characteristics of DAR

The specific enthalpies of the binary solution can be obtained via steam tables or charts at fixed steady states of the binary mixture. They are used to calculate the main energy characteristics of DAR below.

The computational state of the wet vapour after the boiling in the generator is accepted at average concentration of ammonia $\xi_{d'}$ according

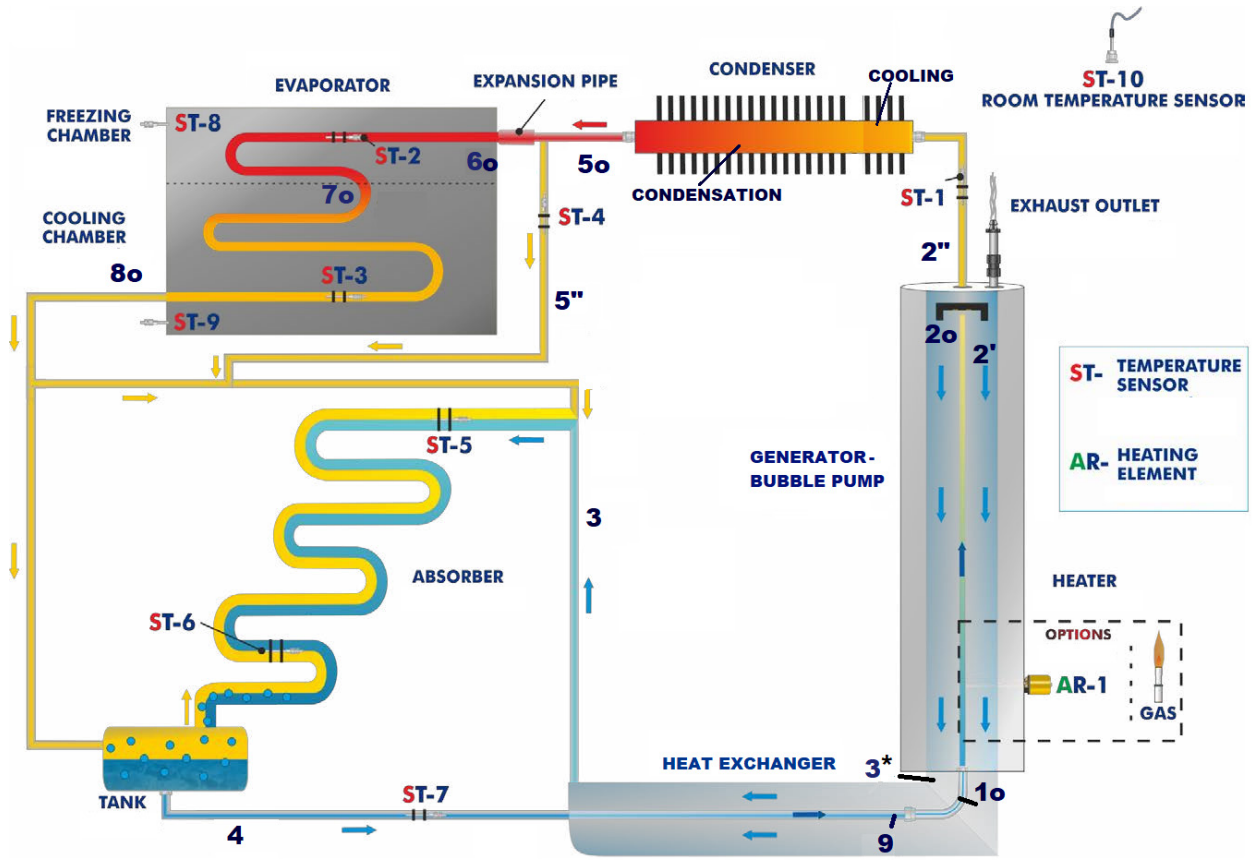

Fig. 1. Scheme of laboratory diffusion absorption refrigeration system TRAB [11, 12].

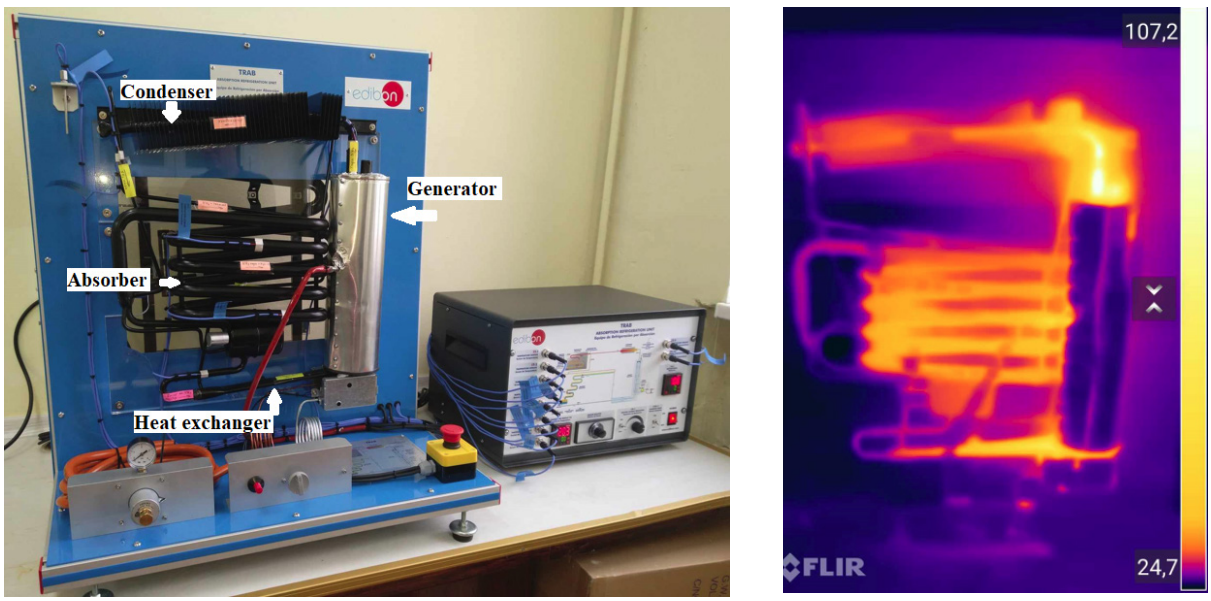

a) b)

Fig. 2. Laboratory unit TRAB (a) and a thermovision of the surface temperatures (b).

to [14] and [15]:

$$\xi_{d'} = \frac{\xi_{rich} + \xi_{poor}}{2} = \frac{\xi_{1'} + \xi_{2'}}{2} \quad (1)$$

where ξ_{rich} and ξ_{poor} are the concentrations of the rich and poor of refrigerant binary solutions at the start and the end of the boiling process, kg NH_3kg^{-1}. They are correspondently equal to $\xi_{1'}$ and $\xi_{2'}$ (Fig. 3).

The circulation ratio f of the generator is the ratio between the mass flows of the inlet rich solution and the outlet vapour:

$$f = \frac{\xi_{d''} - \xi_{poor}}{\xi_{rich} + \xi_{poor}} \quad (2)$$

where $\xi_{d''}$ is the average concentration of the refrigerant in the saturated steam after the boiling in the generator, kg NH_3 kg^{-1}.

The specific heat, exchanged between the rich and poor solutions in the heat exchanger is:

$$q_{he} = (f-1)(h_{2'} - h_3), \text{ kJ kg}^{-1} \quad (3)$$

where $h_{2'}$ and h_3 are the specific enthalpies of the saturated poor liquid solution after the boiling and after the cooling in the heat exchanger, kJ kg^{-1}. A thermal balance of the heat exchanger is used to obtain the specific enthalpy h_1 of the rich liquid solution after the heat exchanger (before the generator). It is used to fix state 1 (1o) on Fig. 3.

$$h_1 = h_4 + \frac{q_{he}}{f}, \text{ kJ kg}^{-1} \quad (4)$$

An auxiliary enthalpy h_o is used for the computation of the specific heats below according to [14] and [15]:

$$h_o = h_{2'} - f(h_{2'} - h_1), \text{ kJ kg}^{-1} \quad (5)$$

The specific heat q_h, consumed by the binary mixture in the generator, is:

$$q_h = h_{d''} - h_o, \text{ kJ kg}^{-1} \quad (6)$$

The specific heat q_c, released at the condensation is obtained by:

$$q_c = h_{d''} - h_5, \text{ kJ kg}^{-1} \quad (7)$$

The specific heat q_a, released at the absorption, is:

$$q_a = h_{8o} - h_o, \text{ kJ kg}^{-1} \quad (8)$$

The specific heat q_e, absorbed at the evaporation (cooling effect), is:

$$q_e = h_{8o} - h_{6o}, \text{ kJ kg}^{-1} \quad (9)$$

The coefficient of performance at cooling is the ratio between the cooling effect and the energy input in the generator:

$$COP_c = \frac{q_e}{q_h} \quad (10)$$

The DAR operates at heat pump mode in a case of utilization of the realized heats at the condensation and absorption (for example for a heating of the room). The coefficient of performance at heating is:

$$COP_c = \frac{q_c + q_a}{q_h} \quad (11)$$

The cooling capacity $\dot{Q}_c$ of the absorption refrigerator can be obtained by:

$$\dot{Q}_c = COP_c . P, \text{ W} \quad (12)$$

where P is the power input of the electrical heater, W.

Absorption cycle at fixed power input

A steady state operation of the laboratory DAR at fixed power input of 80 W is described grapho-analytically to demonstrate the experimental procedures (Table 1). The diffusion absorption cycles is determined in enthalpy-concentration chart of water-ammonia binary mixture on Fig. 3, developed in the University of Stuttgart [13]. The specific enthalpies in Table 1 are approximate as they were read by the enthalpy-concentration chart.

The energy characteristics of DAR, computed by the parameters in Table 1, are given in Table 2. A lower performance at cooling mode and higher

Table 1. Sequence at determination of the absorption cycle at power input of 80 W.

Step	State / process	Way of determination	Parameter	Unit	Value
1	Condensation temperature of ammonia	Measuring and averaging the surface temperatures along the condenser	p_c	°C	31.2
2	Condensation pressure of ammonia	Steam tables of NH_3	p_c	Bar	12.02
3	Evaporation temperature of ammonia	Measuring and averaging the surface temperatures along the cooler part of the evaporator in the freezing chamber	t_e	°C	-0.9
4	Evaporation pressure of ammonia	Steam tables of NH_3	p_e	Bar	4.14
5	State 2' of the saturated liquid after the generator	Reading of the temperature $t_2 = t_{2'} = t_{2''}$ by the sensor ST1. Fixing of Point 2' on Fig. 3 at t_2 and p_c. Reading of the concentration $\xi_{2'}$ and specific enthalpy $h_{2'}$.	p_c	Bar	0.23
			$t_{2'}$	°C	12.02
			$\xi_{2'}$	kg kg^{-1}	125.2
			$h_{2'}$	kJ kg^{-1}	460
6	State 2" of the saturated steam after the generator	The isotherm $t_2 = t_{2'} = t_{2''}$ is constructed in the chart. Fixing of Point 2" on Fig. 3 at $t_{2''}$ and p_c. Reading of the concentration $\xi_{2''}$ and specific enthalpy $h_{2''}$.	$t_{2''}$	°C	125.2
			p_c	Bar	12.02
			$\xi_{2''}$	kg kg^{-1}	0.78
			$h_{2''}$	kJ kg^{-1}	2070
7	State 4 of the subcooled liquid after the absorber	Reading of the temperature t_4 by the sensor ST7. Fixing of Point 4 at t_4 and p_e. Reading of the concentration ξ_4 and specific enthalpy h_4.	ξ_4	kg kg^{-1}	0.52
			p_e	Bar	4.14
			t_4	°C	27
			h_4	kJ kg^{-1}	50
8	State 9 at the start of the boiling	Fixing of Point 9 at $\xi_9 = \xi_4$ and p_c. Reading of the temperature t_9 and specific enthalpy h_9.	t_9	°C	65
			p_c	Bar	12.02
			ξ_9	kg kg^{-1}	0.52
			h_9	kJ kg^{-1}	230
9	State 3* of the poor of refrigerant liquid solution at the inlet of the heat exchanger	Fixing of Point 3* at $\xi_3 = \xi_{2'}$ and p_e. Reading of the temperature t_{3*} and specific enthalpy h_{3*}.	p_e	Bar	4.14
			t_{3*}	°C	83
			$\xi_{2'} = \xi_{3*}$	kg kg^{-1}	0.23
			h_{3*}	kJ kg^{-1}	260
10	State 3 of the poor of refrigerant liquid solution at the inlet of absorber	Reading of the temperature t_3 by the sensor ST5. Fixing of Point 3 at $\xi_3 = \xi_{2'}$ and t_3. Reading of the specific enthalpy h_{3*}.	$t3$	°C	30.3
			$\xi_{2'} = \xi_3$	kg kg^{-1}	0.23
			h_3	kJ kg^{-1}	60
11	State *d'* of the saturated liquid after the generator at average ammonia concentration after the boiling.	Calculation of $\xi_{d'}$ according to eq. (1). Fixing of Point d' on Fig. 3 at $\xi_{d'}$ and p_c. Reading of the temperature $t_{d'}$ and specific enthalpy $h_{d'}$.	$\xi_{d'}$	kg kg^{-1}	0.375
			p_c	Bar	12.02
			$t_{d'} = t_{d''} = t_{do}$	°C	92
12	State d" of the saturated steam after the generator at an average ammonia concentration after the boiling.	The isotherm $t_{d'} = t_{d''} = t_d$ is constructed in the chart. Fixing of Point d" on Fig. 3 at $t_{d''}$ and p_c. Reading of the concentration $\xi_{d'}$ and specific enthalpy $h_{d''}$.	p_c	Bar	12.02
			$t_{d'} = t_{d''} = t_{do}$	°C	92
			$\xi_{d'}$	kg kg^{-1}	0.96
			$h_{d''}$	kJ kg^{-1}	1820

Table 1. Sequence at determination of the absorption cycle at power input of 80 W - *continued*.

13	State 5' of the saturated liquid after the condenser.	Fixing of Point 5' at $\xi_{d''}$ and p_c. Reading of the temperature $t_{5'}$ and specific enthalpy $h_{5'}$.	$\xi_{d''}=\xi_{5'}$	kg kg^{-1}	0.96
			p_c	Bar	12.02
			$t_{5'}$	°C	30
			$h_{5'}$	kJ kg^{-1}	450
14	State 6' of the saturated liquid after the throttling.	Point 5'= Point 6' (equal enthalpies and concentrations)	$h_{6'}$	kJ kg^{-1}	450
15	State 7" of the saturated steam after the evaporation in the freezing chamber.	Fixing of Point 7" on Fig. 3 at $\xi_{7''}$=1 and p_e. The isotherm $t_7 = t_{7'} = t_{7''}$ is constructed. Reading of the temperature $t_{7''}$ and specific enthalpy $h_{7''}$.	pe	Bar	4.14
			$\xi_{7'}$	kg kg^{-1}	1
			$t_7 = t_{7'} = t_{7''}$	°C	-1
			$h_{7''}$	kJ kg^{-1}	1620
16	State 7' of the saturated liquid after the evaporation in the freezing chamber.	Fixing of Point 7' on Fig. 3 at $t_7 = t_{7'} = t_{7''}$ and p_e. Reading of the concentration $\xi_{7'}$ and specific enthalpy $h_{7'}$.	p_e	Bar	4.14
			$\xi_{7'}$	kg kg^{-1}	0.76
			$t_7 = t_{7'} = t_{7''}$	°C	-1
			$h_{7'}$	kJ kg^{-1}	170
17	State 8' of the saturated liquid after the evaporator	Reading of the temperature $t_8 = t_{8'} = t_{8''}$ by the sensor ST3. Fixing of Point 8' at $t_8 = t_{8'} = t_{8''}$ and p_e. Reading of the concentration $\xi_{8'}$ and specific enthalpy $h_{8'}$.	$t_8 = t_{8'} = t_{8''}$	°C	22.8
			$\xi_{8''}$	kg kg^{-1}	0.58
			$h_{8'}$	kJ kg^{-1}	50
			p_e	Bar	4.14
18	State 8o of the wet vapour after the evaporator	The isotherm $t_8 = t_{8'} = t_{8''}$ is constructed. Fixing of Point 8o on Fig. 3 at $t_8 = t_{8'} = t_{8''}$ and $\xi_{d''}$. Reading of the specific enthalpy h_{80}.	$t_8 = t_{8'} = t_{8''}$	°C	22.8
			$\xi_{80} = \xi_{d''}$	kg kg^{-1}	0.96
			h_{8o}	kJ kg^{-1}	1500
			p_e	Bar	4.14
19	State 1 of the rich of refrigerant solution after the heat exchanger (at the inlet of the generator)	Calculation of enthalpy h_1 according to eq. (4). In this case h_1 is an enthalpy of wet vapour $h_1=h_{1o}$ (Fig. 3) Fixing of Point 1o at h_1 and ξ_4.	h_1	kJ kg^{-1}	291
			t_{1o}	°C	68

Table 2. Energy characteristics of DAR.

Circulation ratio f	2.52
Specific heat, exchanged in the heat exchanger q_{he}, kJ kg^{-1}	607
Auxiliary enthalpy h_o, kJ kg^{-1}	35
Specific heat consumption in the generator q_h, kJ kg^{-1}	1785
Specific heat, released at the condensation q_c, kJ kg^{-1}	1370
Specific heat, released at the absorption q_a, kJ kg^{-1}	1465
Specific heat absorbed at the evaporation q_e, kJ kg^{-1}	1050
Coefficient of performance at cooling COP_c	0.59
Coefficient of performance at heating COP_h	1.59
Cooling capacity $\dot{Q}_c$, W	47.05

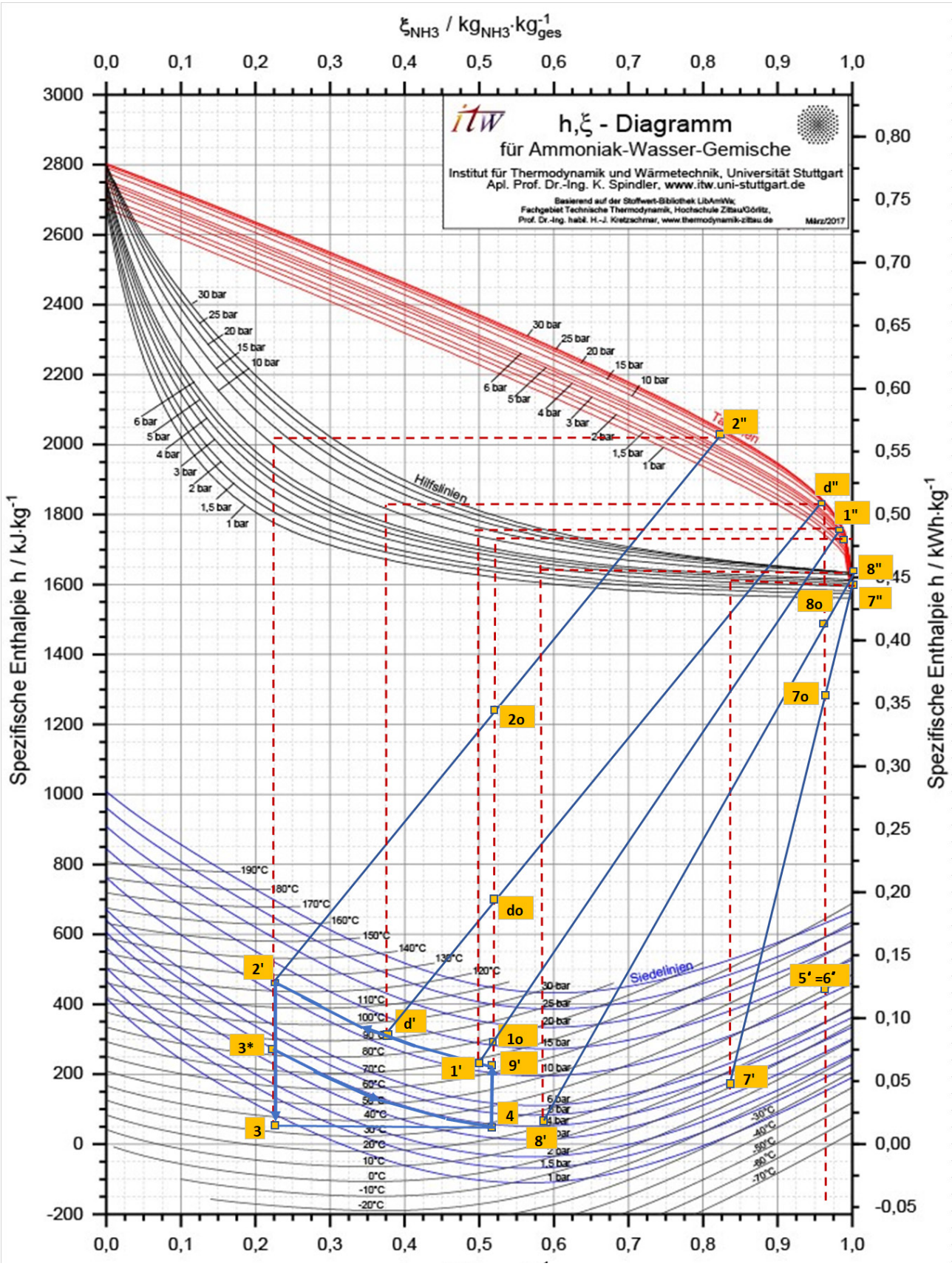

Fig. 3. Diffusion absorption cycle at maximal power input of 80 W.

performance at heat pump mode are established. Therefore, at organizing heat exchange in the condenser and absorber so that the released heat from the binary mixture in these heat exchangers is utilized, the energy gains of the DAR are expected to be higher according to the energy input.

CONCLUSIONS

The proposed methodology allows obtaining of detail information about the thermodynamically states and processes in DAR and estimation of its efficiency. It is useful for the education on the courses of Technical thermodynamic, Thermal techniques, Renewable energy sources, etc. to demonstrate the capabilities and performances of these systems at cooling and heat pump mode. This knowledge is necessary for future engineers in view of the aspirations for a rational use of the available energy resources on a global scale.

Acknowledgements

Authors greatly acknowledge Project КП-06 ПН57/16/ 2021 „Parametric analysis of multiphysical processes in absorption refrigeration systems for efficient utilization of thermal energy ", funded by Bulgarian Ministry of Education and Science, for the assistance of this study.

REFERENCES

1. B.C. Von Platen, C.G. Munters, Refrigerator U.S. Patent 1685764, 1928.
2. M. El-Shafie, M.K. Bassiouny, S. Kambara, S.M. El-Behery, A.A. Hussien, Design of a heat recovery unit using exhaust gases for energy savings in an absorption air conditioning unit, Applied Thermal Engineering, 194, 2021, 117031.
3. B. Yang, Y. Jiang, L. Fu, S. Zhang, Experimental and theoretical investigation of a novel full-open absorption heat pump applied to district heating by recovering waste heat of flue gas, Energy and Buildings, 173, 2018, 45-57.
4. B. Yang, Y. Jiang, L. Fu, S. Zhang, Conjugate heat and mass transfer study of a new open-cycle absorption heat pump applied to total heat recovery of flue gas, Applied Thermal Engineering, 138, 2018, 888-899.
5. Y. Wang, H. Chen, H. Wang, G. Xu, J. Lei, Q. Huang, T. Liu, Q. Li, A novel carbon dioxide capture system for a cement plant based on waste heat utilization, Energy Conversion and Management, 257, 2022, 115426.
6. Z.Y. Xu, H.C. Mao, D.S. Liu, R.Z. Wang, Waste heat recovery of power plant with large scale serial absorption heat pumps, Energy, 165, 2018, 1097-1105.
7. W. Wu, B. Wang, W. Shi, X. Li, Absorption heating technologies: A review and perspective, Applied Energy, 130, 2014, 51-71.
8. Z.Y. Xu, R.Z. Wang, C. Yang, Perspectives for low-temperature waste heat recovery, Energy, 176, 2019, 1037-1043.
9. J. Jeong, H. S. Jung, J. W. Lee, Y. T. Kang, Hybrid cooling and heating absorption heat pump cycle with thermal energy storage, Energy, 283, 2023, 129027.
10. https://www.thermaxglobal.com/product-features/
11. Y. Stoyanov, N. Penkova, K. Krumov, Performance of diffusion absorption refrigerators at variable power input, IOP Conference Series: Earth and Environmental Science, 2024, (in press).
12. Edibon, Practical exercises manual www.edibon.com, 2024
13. K. Spindlerh, ξ-Diagramm für Ammoniak-Wasser-Gemische Institut für Thermodynamik und Wärmetechnik (ITW) Universität, Stuttgart, 2017. www.igte.uni-stuttgart.de
14. T. Todorov, Refrigeration equipment, Techniques Sofia, 1977, (in Bulgarian).
15. T. Todorov, V. Daskalov, Refrigeration exercise manual, Techniques Sofia, 1975, (in Bulgarian).